Structures of *Aquifex aeolicus* KDO8P Synthase in Complex with R5P and PEP, and with a Bisubstrate Inhibitor: Role of Active Site Water in Catalysis[†,‡]

Jian Wang,[§] Henry S. Duewel,[||] Ronald W. Woodard,[||] and Domenico L. Gatti*[,§]

Department of Biochemistry and Molecular Biology, Wayne State University School of Medicine, Detroit, Michigan 48201, and Department of Medicinal Chemistry, College of Pharmacy, University of Michigan, Ann Arbor, Michigan 48109

Received July 6, 2001; Revised Manuscript Received August 17, 2001

ABSTRACT: We have determined the crystal structures of the metalloenzyme 3-deoxy-D-*manno*-octulosonate 8-phosphate (KDO8P) synthase from *Aquifex aeolicus* in complex with phosphoenolpyruvate (PEP) and ribose 5-phosphate (R5P), and with a bisubstrate inhibitor that mimics the postulated linear reaction intermediate. R5P, which is not a substrate for KDO8P synthase, binds in a manner similar to that of arabinose 5-phosphate (A5P), which is the natural substrate. The lack of reactivity of R5P appears to be primarily a consequence of the loss of a water molecule coordinated to Cd^{2+} and located on the *si* side of PEP. This water molecule is no longer present because it cannot form a hydrogen bond with C2-OH^{R5P}, which is oriented in a different direction from C2-OH^{A5P}. The bisubstrate inhibitor binds with its phosphate and phosphonate moieties occupying the positions of the phosphate groups of A5P and PEP, respectively. One of the inhibitor hydroxyls replaces water as a ligand of Cd^{2+}. The current work supports a mechanism for the synthesis of KDO8P, in which a hydroxide ion on the *si* side of PEP attacks $C2^{PEP}$, forming a tetrahedral-like intermediate with a buildup of negative charge at $C3^{PEP}$. The ensuing condensation of $C3^{PEP}$ with $C1^{A5P}$ would be favored by a proton transfer from the phosphate moiety of PEP to the aldehyde carbonyl of A5P to generate the hydroxyl. Overall, the process can be described as a *syn* addition of water and A5P to the *si* side of PEP.

3-Deoxy-D-*manno*-octulosonate (KDO)[1] is an essential component of the lipopolysaccharide (LPS) of all Gram-negative bacteria (*1*). This eight-carbon sugar is the first component of the oligosaccharide core region that links the lipid A moiety of LPS to the O-antigen (*1*). The importance of KDO for cellular homeostasis and growth was first recognized by Rick and Osborn (*2*) with the isolation of a temperature sensitive mutant of *Salmonella typhimurium* defective in KDO synthesis that accumulated incomplete LPS and was severely compromised in DNA, RNA, and protein synthesis (*3*). Characterization of this and other mutant strains of *S. typhimurium* (*4*, *5*) has shown that disruption of LPS through inhibition of KDO synthesis leads to severe alteration of normal growth and function (*6*). This observation, coupled with the fact that KDO is present only in Gram-negative bacteria and plants (*7*), suggests that a valuable chemotherapic strategy may be based on the inhibition of the synthesis and incorporation of KDO into LPS.

The first step in the synthesis of KDO is the condensation of arabinose 5-phosphate (A5P) and phosphoenolpyruvate (PEP) to form KDO 8-phosphate (KDO8P), the phosphorylated precursor of KDO, catalyzed by KDO8P synthase (KDO8PS, EC 4.1.2.16) (*8*). Two distinct classes of KDO8P synthases have been identified differing primarily in the requirement, or lack thereof, of a divalent metal ion for activity (*9*, *10*). We have recently determined the crystal structure of one member of the metal-free class, the *Escherichia coli* enzyme (*11*, *12*), and of one member of the metal-requiring class, the enzyme from the hyperthermophile *Aquifex aeolicus* (*13*). A structural investigation of the *E. coli* enzyme has been reported also by Wagner et al. (*14*) and more recently by Asojo et al. (*15*). In this latter study, both the position of PEP and the mode of binding of a bisubstrate inhibitor were determined. The structure of *A. aeolicus* KDO8PS in complex with various combinations of the natural substrates A5P and PEP and of the activating ion Cd^{2+} (which elicits a 250-fold rate enhancement with respect to the metal-free enzyme; *10*) provides the highest level of definition (1.8 Å resolution) achieved so far for these enzymes (*13*). Of particular note is the fact that since *A. aeolicus* KDO8PS is fully active at 95 °C and has no detectable activity below 30 °C (*16*), a ternary complex with both A5P and PEP could be observed in the crystals, which are stable only below 10 °C.

[†] This research was supported by U.S. Public Health Service Grants AI42868 to D.L.G. and GM53069 to R.W.W. H.S.D. was a recipient of a NSERC (Canada) postdoctoral fellowship.

[‡] The structure factor amplitudes and the refined coordinates of *A. aeolicus* KDO8PS in the complexed states described in this study have been deposited in the Protein Data Bank (entries 1JCX and 1JCY).

* To whom correspondence should be addressed: Department of Biochemistry and Molecular Biology, Wayne State University School of Medicine, Detroit, MI 48201. Telephone: (313) 993-4238. Fax: (313) 577-2765. E-mail: mimo@boatman.med.wayne.edu.

[§] Wayne State University School of Medicine.

[||] University of Michigan.

[1] Abbreviations: KDO, 3-deoxy-D-*manno*-octulosonate; KDO8P, 3-deoxy-D-*manno*-octulosonate 8-phosphate; KDO8PS, 3-deoxy-D-*manno*-octulosonate 8-phosphate synthase; DAH7P, 3-deoxy-D-*arabino*-heptulosonate 7-phosphate; DAH7PS, 3-deoxy-D-*arabino*-heptulosonate 7-phosphate synthase; PEP, phosphoenolpyruvate; A5P, arabinose 5-phosphate; R5P, ribose 5-phosphate; PGL, 2-phosphoglycolate; API, {[(2,2-dihydroxyethyl)(2,3,4,5-tetrahydroxy-6-phosphonooxyhexyl)-amino]methyl}phosphonic acid; rms, root-mean-square; H, helix; S, strand; L, loop.

10.1021/bi015568e CCC: $20.00
Published on Web 11/29/2001

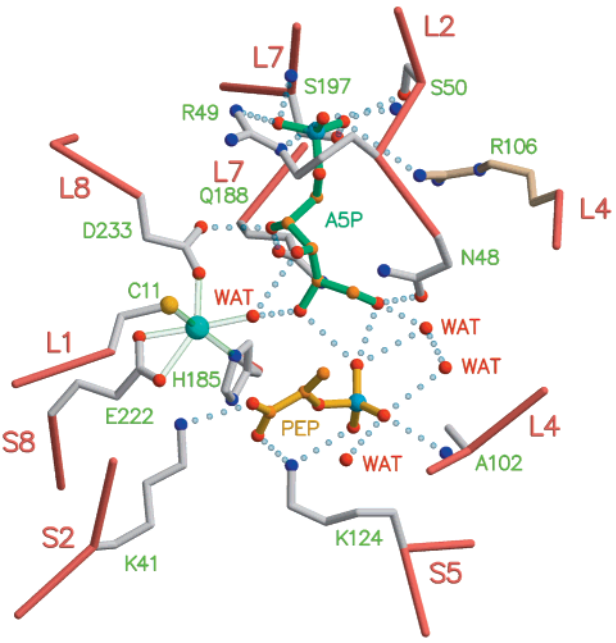

FIGURE 1: *A. aeolicus* KDO8PS active site with A5P and PEP. The Cα trace and side chains of the enzyme are shown with salmon and white bonds, respectively. A single residue, Arg106, originating from a different monomer in the same asymmetric unit, is shown with khaki bonds. The coordination of the Cd^{2+} ion is shown as transparent light green bonds. Hydrogen bonds are shown as transparent dashed light blue lines. Atom colors are as follows: nitrogen, blue; oxygen, red; carbon, orange; sulfur, yellow; phosphorus, pale blue; and cadmium, cyan. PEP is shown as a ball-and-sticks model with gold bonds; the *si* side of PEP is pointing up and to the left, and the *re* side is pointing down and to the right. A5P is shown as a ball-and-sticks model with green bonds; the *re* face of the aldehyde carbonyl is pointing toward the *si* face of PEP. Note the presence of two water molecules, one, which is also a ligand of Cd^{2+}, on the *si* side of PEP and a second on the *re* side, hydrogen bonded to one of the oxygens of the phosphate moiety. These two water molecules are equidistant from $C2^{PEP}$. Coordinates for this figure are from PDB entry 1FWW (*13*).

The general features of the reaction of KDO8P synthesis have been elucidated. The structure of the *A. aeolicus* enzyme in complex with both A5P and PEP (*13*) reveals that PEP binds at the bottom of the active site cleft, with the acyclic aldehyde form of A5P immediately above it (Figure 1). This observation is consistent with the previous finding that 4-deoxy-A5P, which cannot form a ring, is a good substrate for KDO8PS (*17*). PEP and A5P are held in place primarily by interactions of their phosphate moieties with several active site residues. The relative position of the two substrates in the active site confirms earlier evidence that their condensation is stereospecific, involving the addition of the *si* face of $C3^{PEP}$ to the *re* face of the A5P carbonyl (*18*−*20*), and suggests that the reaction leads to the formation of a linear tetrahedral intermediate as originally proposed by Hedstrom and Abeles (*21*) (Scheme 1). In the final step of the reaction, phosphate release occurs by cleavage of the C−O rather than the P−O bond. As a consequence, the anomeric oxygen of the product KDO8P originates from bulk solvent (*18*). This unusual cleavage of the C−O bond has been observed in very few other enzymes, namely, UDP-*N*-acetylglucosamine enolpyruvyl transferase (MurA), 5-enolpyruvylshikimate-3-phosphate (EPSP) synthase, and 3-deoxy-D-*arabino*-heptulosonate 7-phosphate (DAH7P) synthase (*22*, *23*). The reaction catalyzed by DAH7P synthase (DAH7PS, EC 4.1.2.15) is very similar to KDO8P synthesis, requiring the condensation of erythrose 4-phosphate (E4P) and PEP (*24*). The recently determined structure of *E. coli* DAH7PS (*14*, *25*) confirms that KDO8PS and DAH7PS are not only mechanistically but also structurally related, and that they probably originated from a common ancestor. Interestingly, while two different groups or classes of KDO8P synthases have been recognized with respect to their requirement for a metal (*9*), all known bacterial and eukaryotic DAH7P synthases require divalent metals for activity (*26*, *27*). With regard to this point, it is possible that the absence or presence of metal in the active site may be associated with subtle differences in the way the reaction progresses. For example, Asojo et al. (*15*) have proposed that nonmetallo KDO8P synthases form the postulated linear reaction intermediate stepwise via a transient oxocarbenium ion at $C2^{PEP}$ (Scheme 1, path A). In contrast, Duewel et al. (*13*) and Wagner et al. (*28*) favor for both metallo-KDO8PS and DAH7PS an attack by a hydroxide ion on $C2^{PEP}$ with formation of a transient C3 carbanion as originally proposed by Hedstrom and Abeles (*21*) (Scheme 1, path B). In this study, we present new evidence that the latter mechanism is operational in *A. aeolicus* KDO8PS, which is a metallo synthase.

EXPERIMENTAL PROCEDURES

Protein Crystallization and Structure Determination. The A5P−PEP bisubstrate inhibitor {[(2,2-dihydroxyethyl)-(2,3,4,5-tetrahydroxy-6-phosphonooxyhexyl)amino]methyl}-phosphonic acid (abbreviated API in Scheme 1 and Figure 2), containing both the A5P and PEP moieties, was synthesized according to the method of Du et al. (*29*). Crystals of recombinant *A. aeolicus* KDO8PS belonging to space group $P3_121$ ($a = b \cong 84.3$ Å, $c \cong 159.5$ Å) were obtained as described previously (*13*) and incubated in a cryoprotectant holding solution consisting of 100 mM sodium acetate (pH 4.8−4.9), 21% polyethylene glycol 4000, 16% glycerol, 5% ethylene glycol, 100 μM $CdCl_2$, and one or more of the following: 10 mM R5P, 5 mM PEP, and 10 mM API. At the pH of this holding solution, the enzyme is 25% active (H. S. Duewel, unpublished observation). Data sets were collected at 100 K with a R-axis IV image plate detector at the Cu Kα wavelength (Table 1). Oscillation data were processed with HKL (*30*). Model refinement was carried out with CNS version 1.0 using cross-validated maximum likelihood as the target function (*31*). Solvent molecules were added during the final stages of refinement after the protein model had stabilized. Least-squares superpositions were carried out with the program LSQMAN (*32*). Figures were drawn with Molscript (*33*), Bobscript (*34*), and Raster-3D (*35*).

RESULTS

Structure of the Enzyme in Complex with R5P and PEP. R5P and A5P are epimers differing only in the configuration of the C2 chiral center. The C2 hydroxyl of A5P is not expected to be involved in the condensation of A5P and PEP or in the cyclization of the linear intermediate to form KDO8P. Therefore, it is of great interest to understand why R5P is not a substrate for the enzyme while A5P is. Just as A5P forms a ternary complex with PEP in the active site of *A. aeolicus* KDO8PS (*13*), so does R5P (Figure 2A,B). As

Scheme 1: Biosynthesis of 3-Deoxy-d-*manno*-octulosonic Acid (KDO8P) from Arabinose 5-Phosphate (A5P) and Phosphoenolpyruvate (PEP)[a]

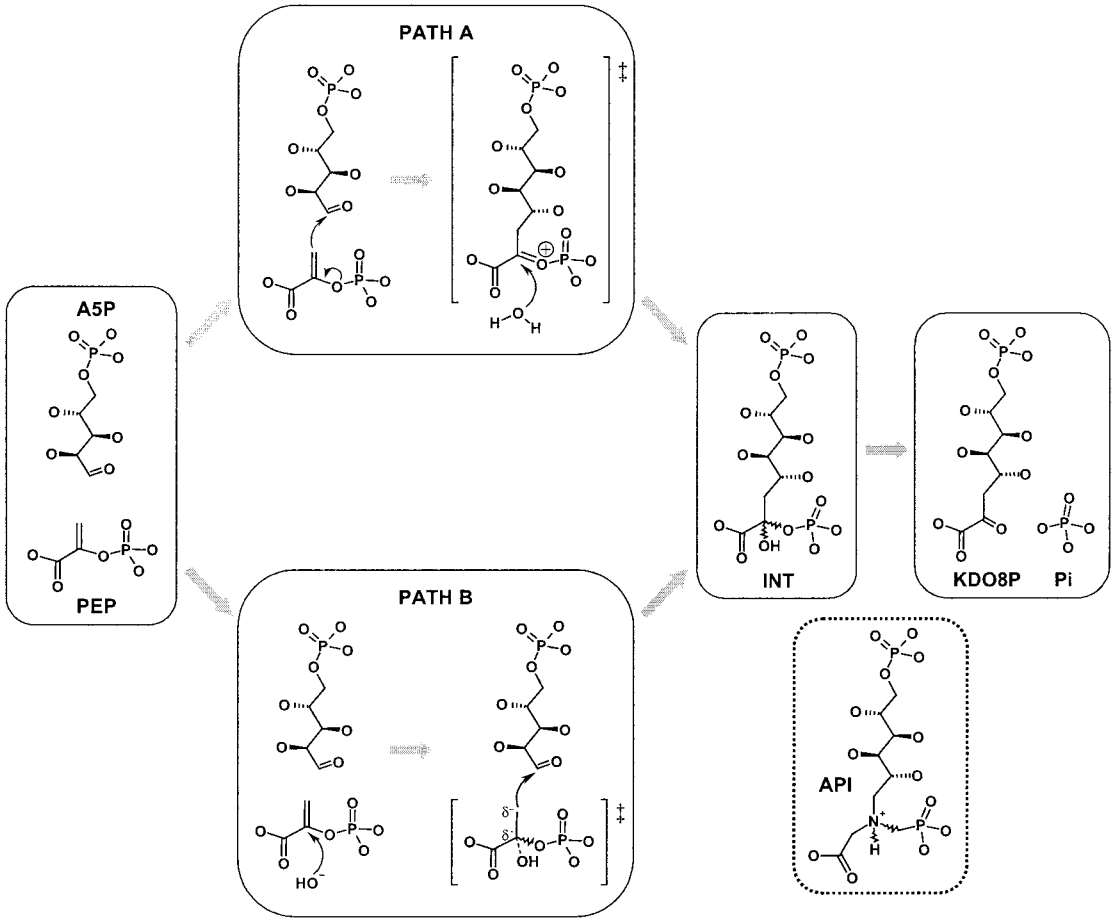

[a] In path A, the postulated linear reaction intermediate (INT) is formed stepwise via a transient oxocarbenium ion at $C2^{PEP}$ that reacts with water. In path B, attack by a hydroxide ion on $C2^{PEP}$ leads to a transient carbanion at $C3^{PEP}$ that reacts with $C1^{A5P}$. The bisubstrate inhibitor (API) is shown in the inset delimited by a dashed line. Transient species are in brackets and are marked with a double daggar (‡) symbol. Only the hydrogens derived from the attacking water or hydroxide ion are shown. Charges on the carboxylate, phosphate, and phosphonate moieties are not shown.

described by Duewel et al. (*13*), A5P binds in the active site of only one of the two molecules of KDO8PS present in the asymmetric unit of the crystal. When this happens, the L7 loop, which is otherwise disordered, closes onto the substrate and seals the active site from the external environment (Figure 1). In addition to interactions between residues of the L7 loop and the phosphate moiety of A5P, a weak hydrogen bond to the bridging oxygen of the A5P phosphate is formed by the guanidinium group of Arg106 belonging to the other molecule of KDO8PS present in the asymmetric unit. All of these interactions are retained when A5P is replaced with R5P. Like A5P, R5P binds only to one of the two molecules of KDO8PS in the asymmetric unit; the other molecule binds only PEP, and a phosphate ion occupies the position corresponding to the phosphate moiety of R5P. Furthermore, in the active site in which R5P binds, the L7 loop is ordered and contributes to stabilizing this substrate analogue (Figure 2A,B). The electron densities for the carbon backbone and the aldehyde carbonyl of R5P are well-defined, and the positions of the hydroxyl groups, although not directly visible, can be inferred on the basis of the known configuration of the chiral centers. As expected from the fact the A5P and R5P are epimers, the most notable difference between these two compounds resides in the orientation of the C2 hydroxyl. When A5P binds, this hydroxyl is hydrogen bonded to a water molecule that is coordinated to the active site Cd^{2+} (Figure 1). In contrast, the C2 hydroxyl of R5P points in a different direction and is not optimally oriented to accept a hydrogen bond from the water molecule coordinated to Cd^{2+} (Figure 2A,B). The loss of this hydrogen bond may be the primary reason this water molecule is not observed in the complex with R5P. In contrast, the water molecule typically located on the *re* side of PEP is present also in the ternary complex with R5P. The distance between $C3^{PEP}$ and $C1^{A5P/R5P}$ is essentially unchanged in the two complexes and therefore is not expected to be a major determinant in explaining the different reactivities of A5P and R5P.

Structure of A. aeolicus KDO8PS in Complex with an Inhibitor Containing both A5P and PEP Moieties. A bisubstrate inhibitor of KDO8PS (API for "$A_{5p}P_{ep}I_{nhibitor}$") mimicking the postulated reaction intermediate (INT in Scheme 1) contains an A5P moiety and a PEP-like moiety that bears a phosphonate instead of a phosphate group and an amine at the position corresponding to $C2^{PEP}$ (*29*). In addition, one extra carbon atom separates the carboxylate group from the amine. With a K_i of 3.3 μM for the *E. coli* enzyme and of 7.0 μM for the *A. aeolicus* enzyme, this compound is among the most potent inhibitors of KDO8PS (*29*; H. S. Duewel, unpublished observation). Overall, the inhibitor fits well in

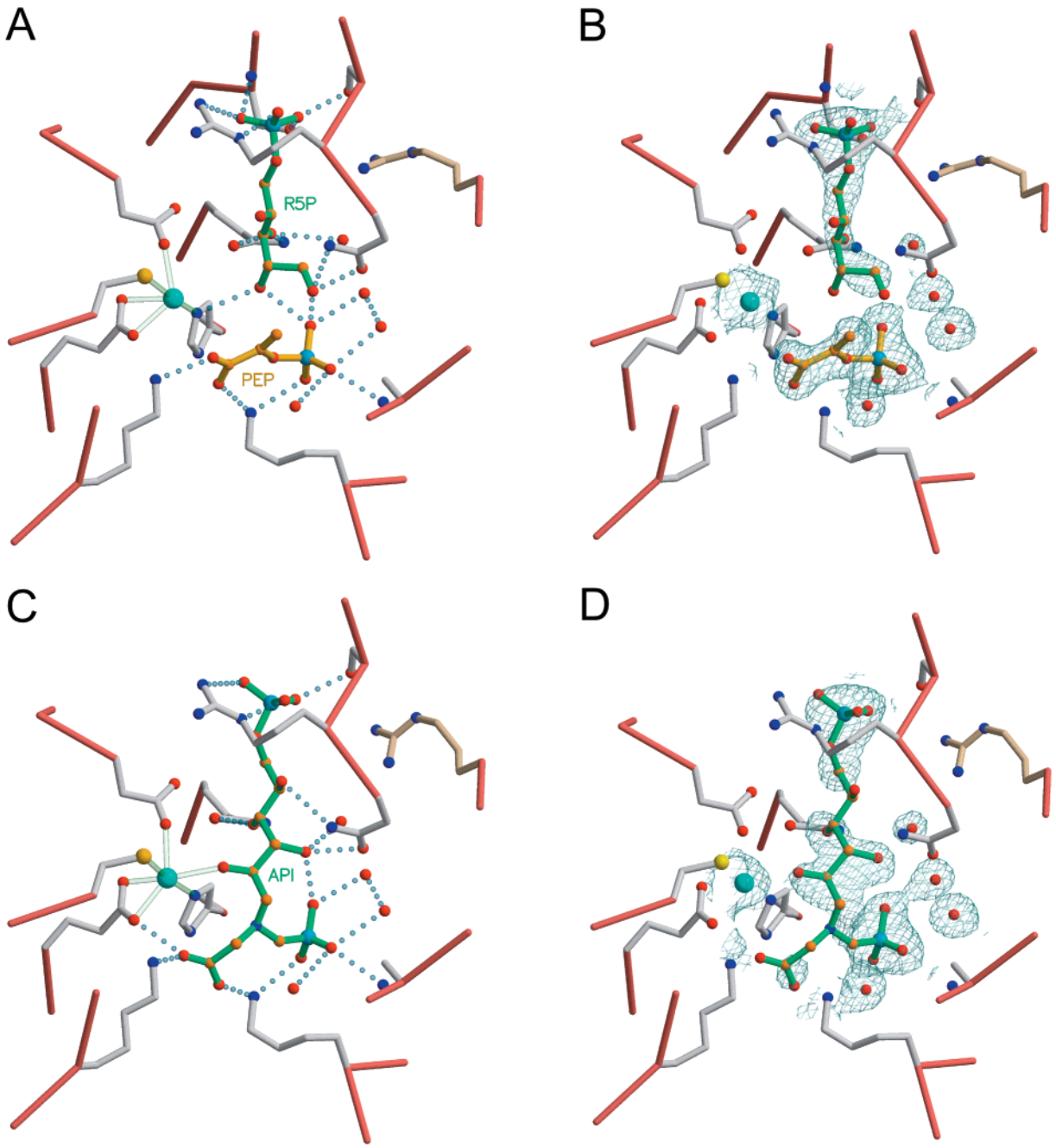

FIGURE 2: *A. aeolicus* KDO8PS active site with R5P and PEP or with a bisubstrate inhibitor. The color coding and viewpoint are the same as in Figure 1. (A) Relative positions of PEP and R5P inside one of the two active sites contained in the asymmetric unit. Note the incomplete octahedral coordination of Cd^{2+} lacking one equatorial ligand (a water molecule that here is missing), with respect to when A5P is bound (Figure 1). (B) SigmaA-weighted omit map of PEP and R5P contoured at 0.9σ with the section of the refined model already shown in panel A. (C) Model for the bisubstrate inhibitor (API) containing both PEP and the A5P moiety. Note the direct coordination of one of the inhibitor hydroxyls to Cd^{2+} and the absence of the additional stabilization of the phosphate moiety of the inhibitor by Ser197, which instead occurs when either A5P (Figure 1) or R5P (panel A) is bound. (D) SigmaA-weighted omit map of the inhibitor contoured at 0.9σ with the section of the refined model already shown in panel C. The electron density of the carboxylate group and of one of the hydroxyls is not well-defined.

an area covering the combined binding sites of A5P and PEP, and its phosphate and phosphonate moieties occupy, respectively, the positions of the phosphate moieties of the two substrates (Figure 2C,D; compare this to Figure 1). Crystals of *A. aeolicus* KDO8PS are maintained in a holding solution at pH 4.8. At this pH, API should be in the form of a quaternary amine (Scheme 1). However, the electron density of the carboxylate group is not well-defined, and therefore, it is not possible to determine unambiguously the nitrogen chirality (the configuration that gives the best fit in the active site is shown in Figure 2). A water molecule is hydrogen bonded to the nitrogen, occupying the same position of a water that in the enzyme with PEP is located on the *re* side of $C2^{PEP}$. In contrast, the water molecule usually located on the *si* side of PEP and coordinated to Cd^{2+} is completely displaced by the hydroxyl group of API that corresponds to the aldehyde carbonyl of A5P. Overall, the active site of the enzyme undergoes only minimal changes to accommodate the inhibitor. The largest changes with respect to the enzyme with bound A5P, or with both A5P and PEP (*13*), are

Table 1: Data Collection and Refinement Statistics[a]

	R5P and PEP	API
data collection		
resolution range (Å)	27−1.9	27−1.8
no. of measurements	419681	837390
no. of unique reflections	46090	58558
⟨redundancy⟩	9.1	14.3
completeness (%)	87.8	94.2
$\langle I\rangle/\sigma\langle I\rangle$	21.4	21.0
R_{merge}[b] (%)	6.6	5.9
refinement		
R_{cryst}[c] (%)	20.2	20.6
R_{free} (%)	23.1	22.9
no. of amino acids	518	509
no. of water molecules	206	228
⟨*B*⟩ (Å^2)	36.7	34.1
σ_A coordinate error (Å)	0.26	0.19
rmsd for bond lengths (Å)	0.005	0.005
rmsd for bond angles (deg)	1.4	1.5
rmsd for dihedrals (deg)	22.5	22.4
rmsd for impropers (deg)	0.81	0.83

[a] For each condition, diffraction data were collected from a single crystal at 100 K. [b] $R_{merge} = \sum_h\sum_i|I(h)_i - \langle I(h)\rangle|/\sum_h\sum_i I(h)_i$, where $I(h)_i$ is the *i*th measurement. [c] $R_{cryst} = \sum|F_{obs} - F_{calc}|/\sum|F_{obs}|$. R_{free} was calculated on 10% of the data omitted from refinement. σ_A coordinate error was calculated with CNS (*36*). Mean *B* values were calculated from the refined models.

observed in the positions of the side chains of His185 and Arg106 and in the residues of the L7 loop. The imidazole ring of His185 moves away from the PEP moiety of API probably to make space for the extra carbon atom connecting the amine and the carboxylate group. The L7 loop is disordered, and Arg106 of the other molecule pulls away from API phosphate moiety (Figure 2C,D). Finally, while A5P binds to only one of the two molecules of the enzyme in the asymmetric unit, the inhibitor binds to both molecules.

DISCUSSION

More than a decade ago, Hedstrom and Abeles (*21*) proposed that the enzymatic condensation of PEP and A5P to form KDO8P proceeds via attack by water at C2^{PEP}, while C3^{PEP} is added to the aldehyde of A5P; this process would yield a linear intermediate (INT in Scheme 1). Recent crystallographic studies of KDO8PS and of the homologous enzyme DAH7PS (*11*, *13*, *14*, *28*) have largely confirmed this hypothesis. However, a recent mechanistic complication has been introduced by the discovery that two classes of KDO8P synthases exist, one requiring metal for activity and one not (*9*, *10*). All known DAH7P synthases require metal, and thus should be equivalent to metallo-KDO8PS. Particular importance has been attributed to the difference between nonmetallo KDO8PS and metallo-DAH7PS by Asojo et al. (*15*), who have proposed that nonmetallo KDO8P synthases form the postulated linear reaction intermediate via a transient oxocarbenium ion at C2^{PEP} (Scheme 1, path A). Water addition at C2 would then be facilitated by the positive charge of the transient intermediate, leading to the formation of a tetrahedral intermediate. In contrast, a reaction path based on an initial attack by water at C2^{PEP} (Scheme 1, path B) would require the formation of a hydroxide ion and is therefore more likely to occur in metallo-KDO8PS and DAH7PS, in which direct coordination of water by the metal would favor its deprotonation. However, Duewel et al. (*13*) have noted that in *A. aeolicus* KDO8PS, a metallo synthase, in addition to a water molecule on the *si* side of C2^{PEP} directly coordinated to the active site metal, there is also a water molecule on the *re* side of C2^{PEP} that might be activated by a nearby base. The structures presented in this study help clarify the role played by these two water molecules in the condensation reaction. When R5P and PEP bind in the active site of *A. aeolicus* KDO8PS, a water molecule is present on the *re* side of PEP, but not on the *si* side (Figure 2A,B). This is possibly the consequence of the fact that the C2 OH group of R5P is pointing in a direction different from that of A5P and is not optimally positioned to stabilize the water molecule on the *si* side of PEP. It is worth noting that the orientation and distance of the aldehyde moieties of R5P and A5P from C3^{PEP} are almost identical. Thus, the absence of the water molecule located on the *si* side of PEP is the most notable effect of the binding of R5P with respect to that of A5P, and appears to be the primary reason for the lack of reactivity of R5P toward PEP. This observation cannot be easily explained with the mechanism postulated by Asojo et al. (*15*), according to which R5P and A5P should be equally reactive toward PEP.

The bisubstrate analogue utilized by Asojo et al. (*15*) with the *E. coli* enzyme, and by us in this study (Figure 2C,D), mimics an intermediate of the reaction immediately antecedent to phosphate release. However, this compound does not appear to bind similarly in the *E. coli* and *A. aeolicus* enzymes. Asojo et al. (*15*) have reported two structures of *E. coli* KDO8PS from crystals maintained in a polyethylene glycol (PEG)-based holding solution, one in complex with PEP (PDB entry IG7U), and one in complex with the bisubstrate inhibitor (PDB entry 1G7V). In both structures, the phosphate moiety of PEP and the phosphonate moiety of the inhibitor occupy approximately the same position. However, this position does not correspond to the position of a sulfate or phosphate ion observed by Radaev et al. (*11*) in the structure of the *E. coli* enzyme from crystals maintained in ammonium sulfate, and interpreted as representing the position of the phosphate moiety of PEP. Interestingly, a superposition of eight different X-ray structures, including *E. coli* KDO8PS as determined by Asojo (*15*), Radaev (*11*), and Wagner (*14*), *A. aeolicus* KDO8PS (ref *13* and this study), and *E. coli* DAH7PS (*25*, *28*), shows that in all except the Asojo structures (corresponding to the P3 cluster in Figure 3), the positions of an isolated sulfate or phosphate ion, of the phosphate moiety of PEP or phosphoglycolate (PGL), and of the phosphonate moiety of API coincide almost perfectly (P1 cluster in Figure 3). Likewise, the positions of an isolated sulfate or phosphate ion and of the phosphate moieties of A5P and API are all close to each other (P2 cluster in Figure 3) with the exception of the Asojo structure of the API inhibitor bound to the *E. coli* enzyme (P4 position in Figure 3). Thus, although internally consistent, the two structures of *E. coli* KDO8PS reported by Asojo appear to be at odds with the structures of KDO8PS from *E. coli* or *A. aeolicus*, and with the structure of the functionally and structurally homologous *E. coli* DAH7PS. It is unlikely that the differences in the observed location of phosphate and of the phosphate or phosphonate moieties of PEP, A5P, or API in the active site of these enzymes are due to differences in the precipitant (PEG or ammonium sulfate) used to obtain and maintain the crystals. For example, the structure of *E. coli* KDO8PS

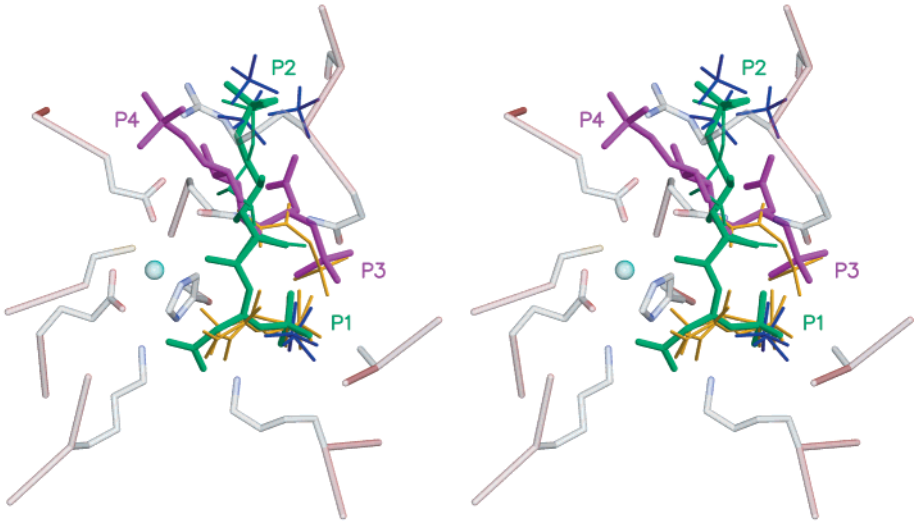

FIGURE 3: Clustering of the binding sites for different ligands in the active sites of KDO8PS and DAH7PS. The Cα traces of the eight independent structures of KDO8PS and DAH7PS were superimposed and the relative positions of the active site ligands determined. They are shown here in stereoview against the common background of *A. aeolicus* KDO8PS (represented in the same orientation as Figure 2, but with transparent bonds). The superimposed ligands are sulfate or phosphate ions (PDB entries 1D9E and 1GG0), PEP (PDB entry 1G7U), and API (PDB entry 1G7V) bound in the active site of *E coli* KDO8PS; PEP and A5P (PDB entry 1FWW) or API [PDB entry 1JCX (this study)] bound in the active site of *A. aeolicus* KDO8PS; and phosphate and PEP (PDB entry 1QR7) or phosphate and PGL (PDB entry 1GG1) bound in the active site of *E. coli* DAH7PS. Isolated phosphate ions are represented with blue bonds, PEP and PGL in gold, and A5P and API in *A. aeolicus* KDO8PS in green; API in *E. coli* KDO8PS is shown in magenta. P1 and P2 mark the positions of phosphate or phosphonate ligands in a group of six consistent structures [PDB entries 1D9E, 1GG0, 1GG1, 1FWW, 1QR7, and 1JCX (this study)]; P3 and P4 mark the positions of phosphate or phosphonate ligands in two outlier structures (PDB entries 1G7U and 1G7V). Least-squares superpositions were calculated with the program LSQMAN (*32*).

reported by Radaev et al. (*11*) was in ammonium sulfate and is consistent with the structure of the *A. aeolicus* KDO8PS in PEG determined by Duewel et al. (*13*). Finally, it should be noticed that the API position as observed by Asojo (Figure 3, magenta trace) is such that the bond between the A5P and PEP moieties of the inhibitor is directed along the bond between C2 and the carboxylate group of PEP rather than along the general direction of the C2−C3 bond, as would be expected if this compound was reporting the correct position of the linear intermediate. In this study, we show that the same bisubstrate inhibitor is instead positioned in the active site of *A. aeolicus* KDO8PS in such a way that its PEP moiety overlaps PEP almost perfectly, and its A5P moiety overlaps A5P, suggesting that the position of the inhibitor in the *A. aeolicus* enzyme may reflect more closely the binding mode of the reaction intermediate (Figure 3, green trace).

What is the likely course of the reaction of KDO8P synthesis as suggested by the studies presented here? The observation that the only significant effect of the binding of R5P is the loss of the water molecule coordinated by Cd^{2+} and the fact that R5P is not a substrate indicate that this water may be essential for the condensation step of the reaction. This water molecule is in van der Waals contact with the *si* face of $C2^{PEP}$, and its coordination to Cd^{2+} is expected to lower its pK_a, favoring deprotonation to a hydroxide ion and the attack on $C2^{PEP}$. The consequent concentration of negative charge at $C3^{PEP}$ would drive the condensation between $C3^{PEP}$ and $C1^{A5P}$. According to this mechanism, the formation of the linear intermediate results from a *syn* addition of water to $C2^{PEP}$ and of $C3^{PEP}$ to $C1^{A5P}$. Since $C1^{A5P}$ and $C3^{PEP}$ are more than 3.0 Å apart in the structure of *A. aeolicus* KDO8PS in complex with PEP and A5P (*13*), some reorientation of the two substrates in the active site must occur to bring the two atoms close enough for bond formation. Significant mobility of A5P in the active site of the enzyme was already noticed by Duewel et al. (*13*): "...the active site (...) allows significant conformational flexibility to A5P. An interesting possibility is that the (...) conformations of A5P reflect the affinity of the enzyme for A5P (or for the chemical groups originating from A5P) at different stages of catalysis. At the start of the reaction, water may be necessary as a simultaneous ligand of the metal and of A5P to favor the formation of a bond between PEP and A5P (...). Once the reaction intermediate is formed, then that part of the molecule that originated from A5P could be stabilized via a direct interaction with the metal." In the panels of Figure 4, we have modeled the minimal positional and conformational changes necessary to convert A5P and PEP into KDO8P and inorganic phosphate following the reaction coordinate postulated in path B of Scheme 1. The positions of the phosphate groups were left unchanged in the various steps of the modeled reaction, because it is clear that these groups represent the primary anchors of the substrates, the intermediate and the product inside the active site (see Figures 1−3). Therefore, any reorientation of the two substrates necessary to bring together the reactive groups was achieved only through modification of the various torsion angles. Panel A of Figure 4 shows the postulated attack onto the *si* side of PEP by a water (colored in red) activated by Cd^{2+}. The predicted relative position of PEP and A5P at the moment of bond formation is such that the 2-OH group of A5P would replace water in the coordination of Cd^{2+} (Figure 4B). At that same instant, the carbonyl of the aldehyde moiety of A5P would be within 2.5 Å of one of the hydroxyls of the phosphate moiety of PEP. As condensation between PEP and A5P must be coupled to conversion of the aldehyde carbonyl to hydroxyl, we propose this might occur via proton transfer from the phosphate group of PEP to the carbonyl oxygen of A5P. Phosphate reproto-

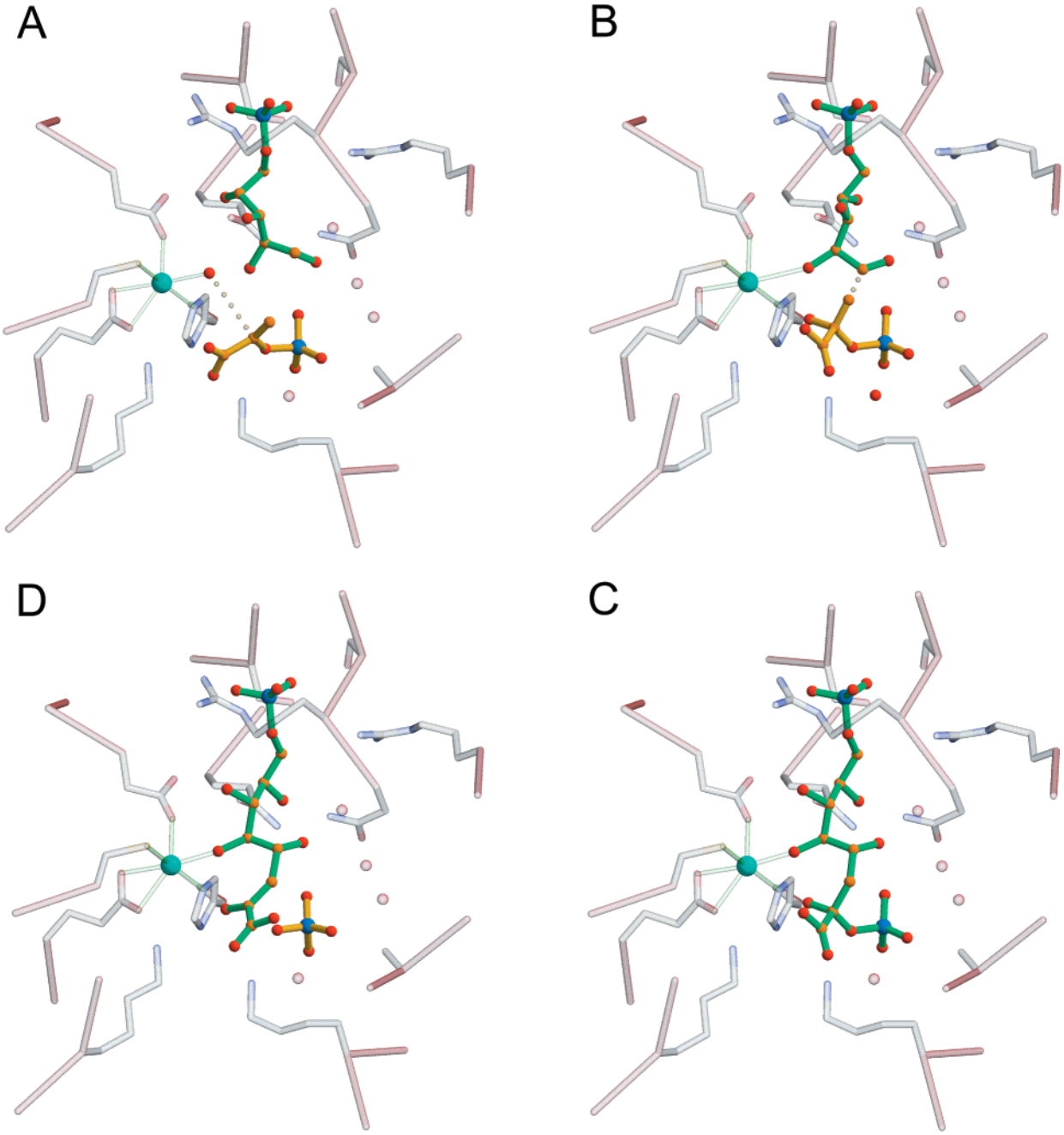

FIGURE 4: Model for KDO8P synthesis. Four snapshots along the reaction coordinate from PEP and A5P to KDO8P were modeled keeping the phosphate groups fixed at their binding sites. Chemical group motions were achieved only through changes in the substrate torsion angles. Active site residues appear as a transparent background; transition state bonds are represented as dashed lines. (A) Reaction starting point. The same experimental coordinates used in Figure 1 (PDB entry 1FWW) are used in this panel; note the water molecule (colored in red) on the *si* side of PEP attacking $C2^{PEP}$. (B) Water attack is complete, generating a tetrahedral center at $C2^{PEP}$ and a buildup of negative charge at $C3^{PEP}$. Reorientation of A5P brings its C2 OH group into the coordination sphere of Cd^{2+} and the aldehyde C1 near $C3^{PEP}$. Note the proximity of the A5P aldehyde carbonyl to one of the phosphate hydroxyls of PEP, which would favor proton transfer to the carbonyl and its conversion to hydroxyl. The water molecule (colored in red) on the *re* side of PEP might reprotonate the phosphate. (C) A bond between $C3^{PEP}$ and $C1^{A5P}$ is formed, producing a linear tetrahedral intermediate (INT of Scheme 1). This intermediate is expected to decay rapidly into KDO8P and inorganic phosphate (D).

nation could then be facilitated by the water molecule (colored in red in Figure 4B) located on the *re* side of PEP. As noticed by Duewel et al. (*13*), this water is stabilized by a network of hydrogen bonds (not shown in Figure 4) that includes one of the hydroxyls of the phosphate moiety of PEP, Asp81 and His83. A chain of hydrogen bonds could be involved in transferring a proton from His83 or Asp81 to the phosphate hydroxyl via this water molecule. Asp81 and His83 are conserved in all known KDO8P synthases, and a glutamic acid is present at the equivalent position of Asp81 in the homologous DAH7P synthases [see the multiple alignment of Radaev et al. (*11*)]. The position of the predicted linear intermediate (INT of Scheme 1) is shown in panel C of Figure 4. The similarity between this model and the experimentally determined binding mode of API (Figure 2C,D) can be easily appreciated. The main difference resides in the fact that with API the hydroxyl attached to C1 of the A5P moiety is coordinated to Cd^{2+}, while in the INT model the hydroxyl attached to C2 of the A5P moiety coordinates the metal. The conformation observed with API can be easily

reached with the INT model by modifying a few torsion angles, and may be part of the subtle changes that are necessary for accommodation of the bisubstrate inhibitor, which is slightly bigger than INT, inside the active site.

One final question remains. If the function of metal in *A. aeolicus* KDO8PS (and in all DAH7P synthases) is to activate a catalytic water, how can nonmetallo KDO8P synthases catalyze the same reaction? In this context, it is probably important that in the *E. coli* enzyme a water molecule is present in almost the same position as the water coordinating Cd^{2+} in the *A. aeolicus* enzyme. In the *E. coli* enzyme, this water is hydrogen bonded to two bases, the ξ-nitrogen of Lys60 and the ϵ-nitrogen of His202, which might favor its deprotonation. However, a more radical view is taken by Asojo et al. (*15*), who propose on the basis of their observation of the position of PEP in the active site of the *E. coli* enzyme, that nonmetallo KDO8PS may work differently from metallo-KDO8PS (see above). There is no explanation at this moment of why the position of PEP observed by these authors in the *E. coli* enzyme is so different from that observed by Duewel et al. (*13*) in the *A. aeolicus* enzyme, and by Shumilin et al. (*25*) in *E. coli* DAH7PS. It is possible, however, that the structures reported by Asojo represent a particular conformational transition that is absent in metallo-KDO8PS. Thus, while evidence is mounting in favor of a direct role by water in the activation of PEP in metallo-KDO8PS, additional studies will be necessary to clarify this point in nonmetallo synthases.

One of the important observations resulting from our studies of *A. aeolicus* KDO8PS (*13*) is that substrate binding controls the opening or closing of the active site to the surrounding environment. When both A5P and PEP are bound, the L7 loop is well-ordered and isolates the active site from bulk solvent. If either A5P alone or PEP alone binds, the loop is not ordered. It was also noticed that A5P (or R5P) binds to only one of the two active sites of the dimer contained in the asymmetric unit. If one considers that the tetramer, which can be generated by application of crystal symmetry, is the native form of the enzyme (*11*−*15*), then it becomes clear that binding of A5P occurs at the active sites located on only one of the two faces of the enzyme (*13*). When A5P binds together with PEP, the associated ordering of the L7 loop also takes place on only one face of the enzyme (*13*). In this study, we showed that the bisubstrate inhibitor binds to both molecules of the enzyme contained in the asymmetric unit and therefore disrupts the normal dialogue between subunits that is the basis for the alternating site/face catalysis of KDO8PS (*13*). Interestingly, when this inhibitor is bound, the L7 loop is not ordered. This observation suggests that the enzyme senses very accurately that condensation between the substrates has occurred and becomes ready to release the product. It will be a challenge for future studies to determine the fine molecular mechanism of this elegant regulatory step.

ACKNOWLEDGMENT

We thank Dr. S. Ackerman for critical evaluation of the manuscript.

REFERENCES

1. Raetz, C. R. (1990) *Annu. Rev. Biochem. 59*, 129−170.
2. Rick, P. D., and Osborn, M. J. (1972) *Proc. Natl. Acad. Sci. U.S.A. 69*, 3756−3760.
3. Rick, P. D., and Osborn, M. J. (1977) *J. Biol. Chem. 252*, 4895−4903.
4. Hansen-Hagge, T., Lehmann, V., and Luderitz, O. (1985) *Eur. J. Biochem. 148*, 21−27.
5. Taylor, W. P., Sheflyan, G. Y., and Woodard, R. W. (2000) *J. Biol. Chem. 275*, 32141−32146.
6. Rick, P. D., and Young, D. A. (1982) *J. Bacteriol. 150*, 456−464.
7. Doong, R. L., Ahmad, S., and Jensen, R. A. (1991) *Plant Cell Environ. 14*, 113−120.
8. Levin, D. H., and Racker, E. (1959) *J. Biol. Chem. 234*, 2532−2539.
9. Birck, M. R., and Woodard, R. W. (2001) *J. Mol. Evol. 52*, 205−214.
10. Duewel, H. S., and Woodard, R. W. (2000) *J. Biol. Chem. 275*, 22824−22831.
11. Radaev, S., Dastidar, P., Patel, M., Woodard, R. W., and Gatti, D. L. (2000) *J. Biol. Chem. 275*, 9476−9484.
12. Radaev, S., Dastidar, P., Patel, M., Woodard, R. W., and Gatti, D. L. (2000) *Acta Crystallogr. D56* (Part 4), 516−519.
13. Duewel, H. S., Radaev, S., Wang, J., Woodard, R. W., and Gatti, D. L. (2001) *J. Biol. Chem. 276*, 8393−8402.
14. Wagner, T., Kretsinger, R. H., Bauerle, R., and Tolbert, W. D. (2000) *J. Mol. Biol. 301*, 233−238.
15. Asojo, O., Friedman, J., Adir, N., Belakhov, V., Shoham, Y., and Baasov, T. (2001) *Biochemistry 40*, 6326−6334.
16. Duewel, H. S., Sheflyan, G. Y., and Woodard, R. W. (1999) *Biochem. Biophys. Res. Commun. 263*, 346−351.
17. Kohen, A., Jakob, A., and Baasov, T. (1992) *Eur. J. Biochem. 208*, 443−449.
18. Dotson, G. D., Dua, R. K., Clemens, J. C., Wooten, E. W., and Woodard, R. W. (1995) *J. Biol. Chem. 270*, 13698−13705.
19. Dotson, G. D., Nanjappan, P., Reily, M. D., and Woodard, R. W. (1993) *Biochemistry 32*, 12392−12397.
20. Kohen, A., Berkovich, R., Belakhov, V., and Baasov, T. (1993) *Bioorg. Med. Chem. Lett. 3*, 1577−1582.
21. Hedstrom, L., and Abeles, R. (1988) *Biochem. Biophys. Res. Commun. 157*, 816−820.
22. Walsh, C. T., Benson, T. E., Kim, D. H., and Lees, W. J. (1996) *Chem. Biol. 3*, 83−91.
23. Floss, H. G., Onerka, D. K., and Carrol, M. (1972) *J. Biol. Chem. 247*, 736−744.
24. De Leo, A. B., and Sprinson, D. B. (1968) *Biochem. Biophys. Res. Commun. 32*, 873−877.
25. Shumilin, I. A., Kretsinger, R. H., and Bauerle, R. H. (1999) *Structure 7*, 865−875.
26. Stephens, C. M., and Bauerle, R. (1991) *J. Biol. Chem. 266*, 20810−20817.
27. Stephens, C. M., and Bauerle, R. (1992) *J. Biol. Chem. 267*, 5762−5767.
28. Wagner, T., Shumilin, I. A., Bauerle, R., and Kretsinger, R. H. (2000) *J. Mol. Biol. 301*, 389−399.
29. Du, S., Faiger, H., Belakhov, V., and Baasov, T. (1999) *Bioorg. Med. Chem. 7*, 2671−2682.
30. Otwinowski, Z., and Minor, W. (1997) *Methods Enzymol. 276*, 307−326.
31. Adams, P. D., Pannu, N. S., Read, R. J., and Brunger, A. T. (1997) *Proc. Natl. Acad. Sci. U.S.A. 94*, 5018−5023.
32. Kleywegt, G. J., and Jones, T. A. (1997) *Methods Enzymol. 277*, 525−545.
33. Kraulis, P. J. (1991) *J. Appl. Crystallogr. 24*, 946−950.
34. Esnouf, R. M. (1997) *J. Mol. Graphics 15*, 132−134.
35. Merrit, E. A., and Murphy, M. E. P. (1994) *Acta Crystallogr. D50*, 869−873.
36. Brunger, A. T., Adams, P. D., Clore, G. M., DeLano, W. L., Gros, P., Grosse-Kunstleve, R. W., Jiang, J. S., Kuszewski, J., Nilges, M., Pannu, N. S., Read, R. J., Rice, L. M., Simonson, T., and Warren, G. L. (1998) *Acta Crystallogr. D54* (Part 5), 905−921.

BI015568E